Adaptive Tube Model Predictive Control for Manipulating Multiple Nanowires with Coupled Actuation in Fluid Suspension

Juan Wu, Kaiyan Yu

Mechanical Engineering Department,
Binghamton University - State University of New York,
Binghamton, NY 13902 USA
(e-mail: jwu123@binghamton.edu, kyu@binghamton.edu)

Abstract: Automated, highly precise online manipulation of multiple nano and microscale objects is essential to achieve scalable nanomanufacturing. One of the biggest limitations of the wireless external actuation is its global and coupled influence in the workspace, which limits the capability to robustly control multiple nano and microparticles independently and simultaneously. Another challenge for the highly precise manipulation of nanoparticles is due to their uncontrolled variations in structures or compositions that result in different dynamic behaviors. In this paper, we present an adaptive tube model predictive control scheme for the simultaneous manipulation of multiple nanowires under coupled electric fields in fluid suspension. The proposed strategy estimates the unknown mobilities of the individual nanowires online, formulates dynamic tubes that update based on the online estimated mobilities and nonlinear dynamics, and addresses the coupled actuation from the global electric field with dynamic separated tubes constructed for each nanowire. Simulations results show that as the number of simultaneously manipulated nanowires increases, the manipulation time increases and the maximum disturbance the system could reject decreases rapidly.

Keywords: Model predictive control; nanowire manipulation; electrophoresis

1. INTRODUCTION

The ability to automatically control microscopic objects is of major interest in various research applications. One of the major challenges in micro and nanoparticles manipulation has been to develop automated systems that are capable of precisely and reliably manipulating multiple objects independently and simultaneously. Such manipulation capabilities will potentially address the scalable manufacture and assembly of functional nanodevices (Yu et al. (2018c,a)). A number of micro and nanomanipulation techniques, such as optical tweezers (Grier (2003)), magnetic tweezers (Gosse and Croquette (2002)), and electric field-based methods (Fan et al. (2011); Yu et al. (2015)), have been introduced to manipulate nanoentities.

In this paper, we focus on electric field-based methods because they are less costly, superior in scalability, and easier to implement for parallel motion control of nanoparticles compared to the other alternatives. With precisely controlled electric fields, electrophoresis (EP) (Yu et al. (2018b)), electro-osmosis (Probst et al. (2012)), and dielectrophoresis (Fan et al. (2011)) could be used as driving forces to steer nanoparticles. Because the EP force is proportional to the electric field strength, it is simple, requires less electric field strength, and is easier to implement for long-range motions for nanowires (Yu et al. (2015)); therefore, EP is used as the driving force to manipulate multiple nanowires. Using electric-field actuation, micro and nanoparticles can be wirelessly and accurately controlled in the workspace (Yu et al. (2015, 2018b,d)). However, the global and coupled nature of the field actuation makes it challenging to control multiple particles individually (Adam et al. (2019)).

Nanowires exhibit uncontrolled variations. Akin et al. (2015) find that the properties of the nanowires with the same composition, fabricated within the same batch, and even from the same sample, may vary by orders of magnitude. Van den Heuvel et al. (2007) show that the electrophoretic mobility of cylindrical-shaped particles is anisotropic. These variations lead to different dynamic behaviors for nanowires suspended in the fluid. To precisely manipulate multiple nanowires, the EP-based manipulation hereby needs a priori knowledge of each particle's effective electrokinetic potential (i.e., the zeta potential) in the suspension. Those uncertainties and variations in the electrophoretic mobility of nanoparticles make the online estimation of the unknown zeta potentials important to manipulate multiple nanowires simultaneously. Instead of independent measurements of the mobilities that use time-consuming instruments or complex calibration processes, we proposed an adaptive control law to steer multiple nanowires to move along the desired trajectories to the targets and estimate the unknown mobilities online in our previous work (Wu and Yu (2019); Wu et al. (2020)). However, the robustness of the system cannot be guaranteed.

In addition to the challenges of coupled actuation from the global field and unknown mobilities of particles, we also

consider the input limitations to stay within the physical capacity of the electric-field actuation. Model Predictive Control (MPC) is considered to address the constrained nonlinear problem of multiple nanowires' manipulation because MPC can incorporate the input constraints (Garcia et al. (1989)). However, MPC relies heavily on the model, which makes it susceptible to external disturbance. Tube MPC is an approximate strategy to address those limitations. A virtual tube is preconstructed offline, together with a robust control law, which keeps the system in the tube. The fix-shaped tube moves along a desired nominal trajectory generated online (Mayne et al. (2006)). However, the tube geometry is restricted for all operating conditions, which can lead to suboptimal performance (Lopez et al. (2019)).

Tube MPC for constrained nonlinear systems was widely investigated in the past decades. An ancillary problem in Mayne et al. (2011) was proposed to provide a local nonlinear control law, whose purpose is to maintain the real state of the uncertain system close to the nominal trajectory. However, this method solves two optimal control problems at each time step; therefore, it requires longer computational time and has increased complexity, especially for the case that incorporates terminal cost function and terminal constraint set. For the system with uncertainties, adaptive control law was combined with the tube MPC approach to capture state-dependent uncertainty in order to potentially reduce the conservativeness of robust MPC while providing robust stability guarantees (Lu and Cannon (2019)). However, Lu's work focuses on the linear time invariant systems and uses a state feedback controller to create the tubes, which cannot be directly applied to the multiple-nanowire manipulation system that is nonlinear and time-varying. Other methods were proposed to estimate the unknown parameters in recent years, such as comparison sets (Aswani et al. (2013)), recursive least square (Heirung et al. (2012)) and set membership identification (Chisci et al. (1998)).

In this paper, we use global electric fields as the external actuation to steer multiple nanowires independently and simultaneously in the fluid channel. The EP force at every nanowire varies due to different zeta potentials and positions of the nanowires. We formulate the problem using nonlinear MPC structure and propose an adaptive tube MPC that estimates the unknown mobilities of the nanowires and addresses the coupled actuation from the global electric field. The main contributions of this work are as follows:

(1) A dynamic tube MPC is proposed to manipulate multiple nanowires with coupled actuation. Instead of constructing a high-dimension tube for the coupled problem, we separate the tube formulation, and construct different lower-dimension tubes for multiple nanowires while still satisfying the coupled actuation for different nanowires. As a result, the computational cost decreases significantly, especially for a large number of nanowires;

(2) The zeta potentials of individual nanowires are estimated online during the control process using the set membership identification method, which makes it possible to manipulate the nanowires without knowing their zeta potential beforehand;
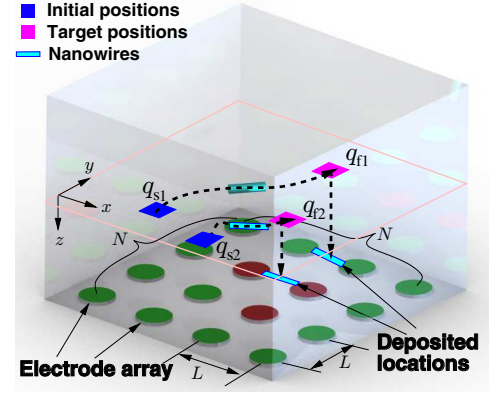
Fig. 1. Schematic of the microfluidic device.

(3) The tube geometry is updated based on the online estimated parameter set and nonlinear dynamics; therefore, the less conservative tubes can be constructed to guarantee the robustness of the system;

(4) The proposed tube MPC is proven to guarantee recursive feasibility and the estimated parameter set shows convergence;

(5) The physical input limitation is considered in the MPC constraints; therefore, multiple nanowires can be steered independently and simultaneously within the physical capacity of the electric-field actuation.

2. PROBLEM FORMULATION

Fig. 1 shows the schematic of the microfluidic device with $N \times N$ lattice-shape distributed electrode array. The circular electrodes with diameter L are fabricated on the bottom substrate with equal distances L between the electrode centers as measured along the x and y axes. Each electrode is independently actuated with DC voltages. The electrode array is covered by a fluid that contains a dilute concentration of nanowires. The precisely controlled electric fields generated by the array of electrodes can be used to control the horizontal motion of suspended nanowires. The nanowire motion is modeled as that of a non-spherical particle immersed in a viscous fluid under an external DC electric field. The motion for an individual nanowire is modeled as follows (Jones (2005)):

$$\dot{\boldsymbol{r}}_i = \begin{bmatrix} v_{ix} \\ v_{iy} \end{bmatrix} = \begin{bmatrix} \zeta_{ix} & \\ & \zeta_{iy} \end{bmatrix} \frac{\varepsilon_\mathrm{m} \boldsymbol{E}_i}{\mu_\mathrm{m}} + \begin{bmatrix} w_{ix} \\ w_{iy} \end{bmatrix}$$
$$= \begin{bmatrix} \zeta_{ix} & \\ & \zeta_{iy} \end{bmatrix} C \begin{bmatrix} E_{ix} \\ E_{iy} \end{bmatrix} + \boldsymbol{w}_i, \tag{1}$$

where the position of the ith nanowire is denoted as $\boldsymbol{r}_i(t) = [x_i(t) \; y_i(t)]^T$, $i = 1, \cdots, n$. $\boldsymbol{E}_i = [E_{ix} \; E_{iy}]^T$ is the DC electric field vector at $\boldsymbol{r}_i$, $C = \varepsilon_\mathrm{m}/\mu_\mathrm{m}$, μ_m is the dynamic viscosity, and ε_m is the electric permittivity. $[\zeta_{ix} \; \zeta_{iy}]$ is the zeta potential of the ith nanowire in x- and y-axis directions, respectively, and will be estimated online for each nanowire. $\boldsymbol{w}_i = [w_ix(t) \; w_iy(t)]^T$ is the bounded external disturbance. $\boldsymbol{E}_i$ can be calculated by superposition of effective electrodes with *unit* voltage and u_j, $j = 1, \cdots, N^2$, is the corresponding voltage that is applied on the $N \times N$ electrode array. From Eq. (1), the electric field is regulated to steer the nanowires' motion by appropriately applying voltage to electrodes.

To formulate the motion equations for all n nanowires, we first re-index the electrodes into a column-wise vector

with N^2 elements. We denote the electric field under unit voltage at $r_i(t)$ by the jth electrode as $E_j(r_i(t)) = [E_{x_j}(r_i(t))\ \ E_{y_j}(r_i(t))]^T$, $i = 1, \cdots, n$, $j = 1, \cdots, N^2$, and the corresponding controlled electrode voltage as $u = \{u_j\} \in \mathbb{R}^{N^2}$. We then concatenate the position vectors of all nanowires as $q(t) = [r_1^T(t) \cdots r_n^T(t)]^T \in \mathbb{R}^{2n}$. By defining a *motion gain matrix*

$$B = C \begin{bmatrix} E_1(r_1(t)) & \cdots & E_{N^2}(r_1(t)) \\ \vdots & \ddots & \vdots \\ E_1(r_n(t)) & \cdots & E_{N^2}(r_n(t)) \end{bmatrix}, \qquad (2)$$

we rewrite Eq. (1) for all nanowires as

$$\dot{q} = \theta B u + w, \qquad (3)$$

where $B \in \mathbb{R}^{2n \times N^2}$, $\theta = \text{diag}[\zeta_{1x}, \zeta_{1y} \cdots \zeta_{nx}, \zeta_{ny}] \in \mathbb{R}^{2n \times 2n}$, and $w \in \mathbb{R}^{2n}$ is the bounded external disturbance. Every two rows in Eq. (3) represent one nanowire's equation of motion. Given the desired target q_f, we want to compute control input u in Eq. (3) that subjected to $u_{\min} \leq u_j \leq u_{\max}$ to steer multiple nanowires to reach their targets, where $u_{\min}$ and $u_{\max}$ are respectively the lower and upper bounds of the applied voltages.

Finally, the system can be formatted as the following nonlinear, discrete-time system by using Euler discretization method with a sampling size of δt:

$$q_{t+1} = A q_t + \theta B(q_t) u_t \delta t + w_t, \qquad (4)$$

in which t is the discrete-time index. The state and input constraints are given by $q_t \in \mathbb{Q}, u_t \in \mathbb{U}$. We assume that the disturbance w_t lies in a convex and compact polytope $\mathbb{W}$, where $\mathbb{W} = \{w_t : F_w w_t \leq f_w\}$. Because θ is a constant matrix to be estimated, we omit the constant time step δt in the following design process for simplicity.

3. ADAPTIVE TUBE MPC

In this section, we first design a parameter estimation scheme that was inspired by Lu and Cannon (2019). Then, a dynamic tube is constructed based on the bound of the external disturbance and the system dynamics. Due to the coupled actuation from the electric fields, we construct the tubes for multiple nanowires under the coupled, limited input. For each nanowire, we build a tube individually using the same constrained input set. During the tube construction process for the multiple nanowires, the open-loop reference trajectories are designed online by the nominal system.

3.1 Parameter Estimation

At time step t, the current state q_t can be observed by the position feedback from the microscope camera. A polytopic set of possible parameters, denoted by Δ_t, can be determined by the known current system state and the previous-step state. According to Eq. (4), we obtain $w_{t-1} = q_t - (A q_{t-1} + \theta B(q_{t-1}) u_{t-1}) \in \mathbb{W}$. We then build the auxiliary set Δ_t calculated from disturbance bound.

$$\begin{aligned} \Delta_t &= \{\theta : q_t - (A q_{t-1} + \theta B(q_{t-1}) u_{t-1}) \in \mathbb{W}\} \\ &= \{\theta : F_w(q_t - (A q_{t-1} + \theta B(q_{t-1}) u_{t-1})) \leq f_w\} \\ &= \{\theta : F_w(q_t - A q_{t-1}) - F_w \theta B(q_{t-1}) u_{t-1} \leq f_w\} \\ &= \{\theta : -F_w \theta B(q_{t-1}) u_{t-1} \leq f_w - F_w(q_t - A q_{t-1})\}. \end{aligned} \qquad (5)$$

Because θ is a diagonal matrix, by setting $F_{\theta t} = -F_w \text{diag}(B(q_{t-1}) u_{t-1})$ and $f_{\theta t} = f_w - F_w q_t + F_w A q_{t-1}$, Eq. (5) can be rewritten as $\Delta_t = \{\theta : F_{\theta t} \theta \leq f_{\theta t}\}$. After constructing this polytopic set, we design the updating law for the unknown parameters set. We initialize the estimated parameter set to be $\Theta_0 = \{\theta : F_0 \theta \leq f_0\}$, and at each time step t, denote the estimated parameter set as $\Theta_t = \{\theta : F_t \theta \leq f_t\}$, where F_t and f_t are updating online. We update the parameters set by $\Theta_t = \Theta_{t-1} \cap \Delta_t$. With the updating law, for all $t \in \mathbb{N}$, it holds that $\Theta_{t+1} \subseteq \Theta_t$.

3.2 Optimized Dynamic Tubes

Next, we derive the cross sections for the dynamic tubes. Although the system in Eq. (4) is nonlinear, at time step t, $B(q_t)$ is a fixed matrix, and we choose θ to be the largest vertex of the above estimated parameters set. Therefore, the system can be linearized around the current state at each time step. The problem then becomes constructing tubes for a linear system at every step as the system updates. To construct the tube for every single nanowire, we consider the system equation for each nanowire.

$$q_{t+1}^i = A^i q_t^i + \theta^i B^i(q_t^i) u_t + w_t^i, \qquad (6)$$

in which A^is are 2×2 identity matrices, q_t^i represents the state of ith nanowire, $i = 1, \cdots, n$, $\theta^i = \text{diag}[\zeta_{ix}, \zeta_{iy}]$ are the estimated zeta potential values for ith nanowire, and $B^i(q_t^i)$ is the $(2i-1)$th to $(2i)$th rows of $B(q_t)$ matrix for $i = 1, \cdots, n$. Note that we use the separate equation of motion for each nanowire to construct its own tube, but the input u_t is coupled for all the nanowires. Therefore, the tube formulation is separated for each nanowire and the feedback control law and related input constraint set are identical for all the nanowires.

For the ith nanowire, let $M_j^i \in \mathbb{R}^{n \times N^2}$, $j \in \mathbb{N}$, and choose $k \geq 2$ to define $M_k^i \triangleq [M_0^i, M_1^i, \cdots, M_{k-2}^i, M_{k-1}^i]^T$. An appropriate characterization of a family of robust control invariant (RCI) sets for the *unconstrained ith* nanowire's motion system is given by the following expression:

$$R_k^i(M_k^i) \triangleq \bigoplus_{m=0}^{k-1} D_m^i(M_k^i) \mathbb{W}, \qquad (7)$$

where $\bigoplus$ represents the Minkowski sum of the sets. The matrices $D_m^i(M_k^i)$ are defined as $D_0^i(M_k^i) \triangleq I$ and $D_m^i(M_k^i) \triangleq (A^i)^m + \sum_{j=0}^{m-1} (A^i)^{m-1-j} \theta_{\text{est}}^i B^i(q_t^i) M_j^i$ for $m \geq 1$, where θ_{est}^i is the estimated zeta potential value for the ith nanowire and M_j^i is the jth element in M_k^i.

Next, we design a feedback law ν that keeps the states in the tubes. To solve for ν that can completely reject the *current* disturbance effect in k time steps, the M_k^i should satisfy the following constraint:

$$D_k^i(M_k^i) = 0. \qquad (8)$$

From the controllability of the system for each nanowire and the full rank of the couple $[A^i,\ \ \theta^i B^i(q_t^i)]$ being 2, there always exists such M_k^i that satisfies Eq. (8) by selecting $k \geq 2$.

Because of the coupled actuation for multiple nanowires, when we compute the feedback law ν, the coupled effect

from the ith nanowire's input to the jth nanowire could be avoided by setting $\boldsymbol{M}_k^i$ to satisfy the constraints

$$\boldsymbol{B}^i(\boldsymbol{q}_t^i)\boldsymbol{M}_k^j = \boldsymbol{0}, \text{ when } i \neq j. \tag{9}$$

Denote all $\boldsymbol{M}_k^i$ that satisfy the conditions in Eqs. (8) and (9) by $\mathbb{M}_k \triangleq [\boldsymbol{M}_k^1, \boldsymbol{M}_k^2, \cdots, \boldsymbol{M}_k^n]$.

We can solve a quadratic programming problem to define a feedback control law $\boldsymbol{\nu}$, which makes the sets $\boldsymbol{R}_k^i(\boldsymbol{M}_k^i)$ be RCI sets for the system in Eq. (6). The quadratic programming problem is formulated as $\boldsymbol{w}^{i^*} \triangleq \arg\min_{\boldsymbol{w}^i}\{\|\boldsymbol{w}^i\|^2 \mid \boldsymbol{w}^i \in \boldsymbol{W}(\boldsymbol{q}_t^i)\}$, and $\boldsymbol{W}(\boldsymbol{q}_t^i) \triangleq \{\boldsymbol{w}^i \mid \boldsymbol{w}^i \in \mathbb{W}^k, \boldsymbol{D}^i\boldsymbol{w}^i = \boldsymbol{q}_t^i, i = 1, 2 \cdots n\}$, where $\mathbb{W}^k \triangleq \underbrace{\mathbb{W} \times \cdots \times \mathbb{W}}_{k}$ and $\boldsymbol{D}^i = [\boldsymbol{D}_{k-1}^i(\boldsymbol{M}_k^i), \cdots, \boldsymbol{D}_0^i(\boldsymbol{M}_k^i)]$. Then $\boldsymbol{\nu}$ can be defined as

$$\boldsymbol{\nu}^*(\boldsymbol{q}_t) \triangleq [M_{k-1}^1, \cdots, M_0^1]\boldsymbol{w}^{1^*} + [M_{k-1}^2, \cdots, M_0^2]\boldsymbol{w}^{2^*}$$
$$+ \cdots + [M_{k-1}^n, \cdots, M_0^n]\boldsymbol{w}^{n^*}. \tag{10}$$

The tube sets $\boldsymbol{R}_k^i(\boldsymbol{M}_k^i)$ and the feedback control law $\boldsymbol{\nu}$ are parameterized by $\boldsymbol{M}_k^i$, and a suitable $\boldsymbol{M}_k^i$ can be obtained by solving the following optimization problem:

$$\overline{\mathbb{P}}_k : (\boldsymbol{M}_k^{i^*}, \alpha_1^*, \cdots, \alpha_n^*, \beta^*) = \underset{\boldsymbol{M}_k^i, \alpha_i, \beta}{\arg\min} \quad \delta$$

$$\text{subject to} \quad \boldsymbol{M}_k^i \in \mathbb{M}_k, \ \boldsymbol{R}_k^i(\boldsymbol{M}_k^i) \subseteq \alpha_i \mathbb{Q},$$
$$\boldsymbol{U}^i(\boldsymbol{M}_k^i) \subseteq \beta\mathbb{U}, \ \alpha_i \in [0,1], \beta \in [0,1],$$
$$\sum_1^n q_{\alpha i}\alpha_i + q_\beta\beta \leq \delta, \ i = 1, \cdots, n,$$

where $\boldsymbol{R}_k^i(\boldsymbol{M}_k^i)$ is defined by Eq. (7), $\boldsymbol{U}^i(\boldsymbol{M}_k^i) \triangleq \bigoplus_{m=0}^{k-1} M_m^i \mathbb{W}$, $q_{\alpha 1}, \cdots, q_{\alpha n}$ reflect the contraction of each tube, respectively, and q_β reflects the contraction of the control constraint set.

The solution $\boldsymbol{M}_k^{i^*}$ to the above optimization problem $\overline{\mathbb{P}}_k$ yields a set of tube sets $[\boldsymbol{R}_k^{1^*}(\boldsymbol{M}_k^1), \cdots, \boldsymbol{R}_k^{n^*}(\boldsymbol{M}_k^n)]$, where $\boldsymbol{R}_k^{i^*}(\boldsymbol{M}_k^i) \triangleq \boldsymbol{R}_k^i(\boldsymbol{M}_k^{i^*}), \ i = 1, \cdots, n$, and the feedback control law $\boldsymbol{\nu}^*(\boldsymbol{q}_t) \triangleq [M_{k-1}^{1^*}, \cdots, M_0^{1^*}]\boldsymbol{w}^{1^*} + \cdots + [M_{k-1}^{n^*}, \cdots, M_0^{n^*}]\boldsymbol{w}^{n^*}$ that satisfies

$$\boldsymbol{R}_k^{i^*}(\boldsymbol{M}_k^i) \subseteq \alpha_i^*\mathbb{Q}, \ i = 1, \cdots, n,$$
$$\boldsymbol{\nu}^*(\boldsymbol{q}_t) \in \boldsymbol{U}(\mathbb{M}_k) \subseteq n\beta^*\mathbb{U}, \tag{11}$$

where $\boldsymbol{U}(\mathbb{M}_k) \triangleq \bigoplus_{i=1}^n \boldsymbol{U}^i(\boldsymbol{M}_k^i)$.

Lemma 1. For the ith nanowire, given any $\boldsymbol{M}_k^i$ satisfies the constraints in Eqs. (8) and (9), $k \geq 2$ and the corresponding set $\boldsymbol{R}_k^i(\boldsymbol{M}_k^i)$, the feedback control law computed from Eq. (10) exists such that $\boldsymbol{A}^i\boldsymbol{q}_t^i + \boldsymbol{\theta}_{\text{est}}^i\boldsymbol{B}^i(\boldsymbol{q}_t^i)\boldsymbol{\nu}(\boldsymbol{q}_t^i) \bigoplus \mathbb{W} \subseteq \boldsymbol{R}_k^i(\boldsymbol{M}_k^i), \forall \boldsymbol{q}_t^i \in \boldsymbol{R}_k^i(\boldsymbol{M}_k^i)$, i.e., the set $\boldsymbol{R}_k^i(\boldsymbol{M}_k^i)$ is the RCI set for the separated system $\boldsymbol{q}_{t+1}^i = \boldsymbol{A}^i\boldsymbol{q}_t^i + \boldsymbol{\theta}^i\boldsymbol{B}^i(\boldsymbol{q}_t^i)\boldsymbol{u}_t + \boldsymbol{w}_t^i$ and constraint sets $\mathbb{Q}, \mathbb{U},$ and $\mathbb{W}$.

Proof. See Appendix A.

3.3 Nominal System Controller

The nominal trajectory is the central path of the tubes that is generated by the nominal system defined as $\boldsymbol{z}_{t+1} = \boldsymbol{A}\boldsymbol{z}_t + \boldsymbol{\theta}_{\text{est}}\boldsymbol{B}(\boldsymbol{z}_t)\boldsymbol{v}_t$, where $\boldsymbol{z}$ is the state of the nominal system, and $\boldsymbol{v}$ is the input of the nominal system. First,

we define a set $\boldsymbol{R}_k(\boldsymbol{q}_t^1, \cdots, \boldsymbol{q}_t^n) \triangleq \{(\boldsymbol{q}_t^i \mid \boldsymbol{q}_t^i \in \boldsymbol{R}_k^i(\boldsymbol{M}_k^i), i = 1, \cdots, n\}$. Together with the input constraint shown in Eq. (11), we define the sets $\mathbb{Z} \triangleq \mathbb{Q} \ominus \boldsymbol{R}_k(\boldsymbol{q}_t), \mathbb{V} \triangleq \mathbb{U} \ominus n\beta^*\mathbb{U}$ to be the state and input constraint sets for the nominal system, respectively, to ensure the robustness of the system in Eq. (3). The $\ominus$ represents the Minkowski difference between the sets. Now we can solve a finite-horizon, optimal control problem for the nominal trajectory, which is defined by

$$\min_{\boldsymbol{z}, \boldsymbol{v}} \quad \sum_{k=0}^{N_h-1} (\|\boldsymbol{z}_k - \boldsymbol{q}_f\|_Q^2 + \|\boldsymbol{v}_k\|_R^2),$$
$$\text{subject to} \quad \boldsymbol{z}_{k+1} = \boldsymbol{A}\boldsymbol{z}_k + \boldsymbol{\theta}_{\text{est}}\boldsymbol{B}(\boldsymbol{z}_k)\boldsymbol{v}_k, \tag{12}$$
$$\boldsymbol{z}_k \in \mathbb{Z}, \boldsymbol{v}_k \in \mathbb{V}, \boldsymbol{z}_{N_h} \in \mathbb{Z}_f,$$

where $\boldsymbol{q}_f$ is the state that contains the target positions of the nanowires, Q and R are positive definite matrices with suitable dimensions, N_h is the prediction horizon, $\mathbb{Z}_f$ is the terminal set, which is chosen to be the maximal positively invariant set Raković and Villanueva (2017) for $\boldsymbol{z}_{t+1} = (\boldsymbol{A} + \boldsymbol{\theta}_{\text{est}}\boldsymbol{B}(\boldsymbol{z}_t)K)\boldsymbol{z}_t$ with constraints $\mathbb{Z}$ and $\mathbb{V}$, and $\|\boldsymbol{z}_k - \boldsymbol{q}_f\|_Q^2 = (\boldsymbol{z}_k - \boldsymbol{q}_f)^{\mathrm{T}}Q(\boldsymbol{z}_k - \boldsymbol{q}_f), \|\boldsymbol{v}_k\|_R^2 = \boldsymbol{v}_k^{\mathrm{T}}R\boldsymbol{v}_k$. The optimal problem gives a state sequence and control sequence shown as follows: $\boldsymbol{Z}^*(\boldsymbol{q}_t) = [\boldsymbol{z}_0^*(\boldsymbol{q}_t), \boldsymbol{z}_1^*(\boldsymbol{q}_t), \cdots, \boldsymbol{z}_{N_h}^*(\boldsymbol{q}_t)]$, and $\boldsymbol{V}^*(\boldsymbol{q}_t) = [\boldsymbol{v}_0^*(\boldsymbol{q}_t), \boldsymbol{v}_1^*(\boldsymbol{q}_t), \cdots, \boldsymbol{v}_{N_h-1}^*(\boldsymbol{q}_t)]$.

With the above solutions, the corresponding optimal dynamics tube $\boldsymbol{Q}^i(\boldsymbol{q}_t^i)$ for the ith nanowire and the control policy $\boldsymbol{u}_t$ are defined as below, respectively:

$$\boldsymbol{Q}^i(\boldsymbol{q}_t^i) \triangleq \boldsymbol{z}_0^*(\boldsymbol{q}_t^i) \bigoplus \boldsymbol{R}_k^i(\boldsymbol{M}_k), \ i = 1, \cdots, n \tag{13}$$

$$\boldsymbol{u}_t \triangleq \boldsymbol{v}_0^*(\boldsymbol{q}_t) + \boldsymbol{\nu}^*(\boldsymbol{q}_t). \tag{14}$$

Lemma 2. Given the proposed control law $\boldsymbol{u}_t$ in Eq. (14), the actual state $\boldsymbol{q}_t$ of the system in Eq. (4) satisfies $\boldsymbol{q}_t^i \in \boldsymbol{Q}^i(\boldsymbol{q}_t^i), \ i = 1, \cdots, n$ for all the time t.

Proof. For ith nanowire, $\boldsymbol{v}_0^*(\boldsymbol{q}_t)$ leads to the state $\boldsymbol{z}_0^*(\boldsymbol{q}_t^i)$, and according to Lemma 1, $\boldsymbol{\nu}^*(\boldsymbol{q}_t)$ always keeps the state in the tube $\boldsymbol{R}_k^i(\boldsymbol{M}_k)$. From the definition of $\boldsymbol{Q}^i(\boldsymbol{q}_t^i)$ in Eq. (13) and the control law $\boldsymbol{u}_t$ in Eq. (14), the control law can make the state of ith nanowire satisfy $\boldsymbol{q}_t^i \in \boldsymbol{Q}^i(\boldsymbol{q}_t^i)$. This completes the proof.

4. SIMULATION RESULTS

In this section, we show the simulation results of controlling multiple nanowires in a 4×4 electrodes array microfluidic device with $L = 600 \ \mu m$. The dynamic system is discretized by a step size of 0.1 s. The input voltages applied to each electrode are limited within $[-600, 600]$ V. All the nanowires are restricted in the workspace, i.e., each nanowire's state bounds by $[0, 1800] \ \mu m$. The parameter matrices Q and R in the cost function (12) are set as $Q = I \in \mathbb{R}^{2n \times 2n}$, $R = I \in \mathbb{R}^{N^2 \times N^2}$, and the prediction horizon is $N_h = 10$. In the simulation, we set a *target area* for each nanowire, which is a ball centered at the target points with a radius of 5 μm. When all the nanowires locate inside their corresponding target areas, we assume that the manipulation is complete.
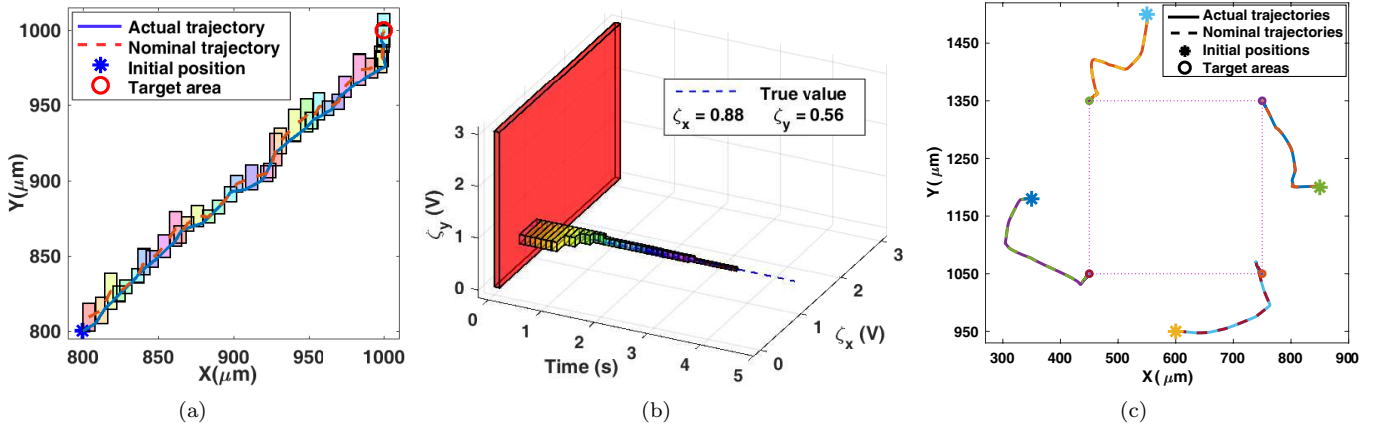
Fig. 2. (a) Trajectories for manipulating one nanowire. The color shaded areas are the dynamic tubes. (b) Zeta-potential set estimation for one nanowire. (c) Trajectories for manipulating four nanowires to form a square pattern.

First, we manipulate one nanowire from the starting position to its target area. Assume the true values of the zeta potentials are $[\zeta_x, \zeta_y] = [0.88, 0.56]$ V, and the initial guesses are $[3, 3]$ V. The disturbance bound is $w \in \mathbb{W} \triangleq \{w \in \mathbb{R}^2 \mid |w|_\infty \leq 5 \ \mu m\}$. Compared to the motion of the nanowire, the disturbance bound is 48% of the maximum state change in one step. Fig. 2(a) shows the trajectories and tubes for the nanowire. Fig. 2(b) shows the updated set for the unknown zeta potentials at different time steps. Under the large disturbance bound, the zeta potential set converges to a small set around the true value with ±9% accuracy in 2.5 s, and the total manipulation time is 3.6 s.

Next, we simultaneously steer multiple nanowires to their independent targets using the proposed control scheme. Fig. 2(c) shows the result of manipulating four nanowires to form a square pattern. The true zeta potentials of the nanowires are $[\zeta_{1x}, \zeta_{1y}] = [0.88, 0.56]$ V, $[\zeta_{2x}, \zeta_{2y}] = [0.73, 0.66]$ V, $[\zeta_{3x}, \zeta_{3y}] = [0.91, 0.82]$ V, and $[\zeta_{4x}, \zeta_{4y}] = [0.92, 0.76]$ V, and the initial guesses are 3 V for all the zeta potentials. The disturbance bound is $w \in \mathbb{W} \triangleq \{w \in \mathbb{R}^2 \mid |w|_\infty \leq 0.02 \ \mu m\}$. Compared to the motion of the nanowires, the disturbance bound is 0.5% of the maximum state change in one step. The zeta potential estimation results rapidly converge to the neighborhood of the true values within 2.5 s with ±0.2% accuracy, while the total manipulation time of the four simultaneous nanowires increases to 123.7 s.

Table 1. Comparison of the maximum disturbance bound and the total manipulation time for different numbers of nanowires

Number of nanowires	1	2	3	4
Ratio of the disturbance	48%	13%	1.5%	0.5%
Manipulation time (s)	3.6	7.7	33.6	123.7

Finally, we evaluate the maximum disturbance under constraint satisfaction by using the shooting method with different numbers of nanowires. Table 1 shows the ratio of the maximum disturbance bound to nanowires' maximum motion in one step and the total manipulation time with those maximum disturbance bounds. From the comparison, the disturbance that the system can reject decreases exponentially and the manipulation time increases rapidly with an increase in the number of nanowires. In addition,

the maximum disturbance is also related to the relative position between the nanowires. The closer the nanowires are, the smaller external disturbance the system can reject.

5. CONCLUSION

In this paper, we proposed an adaptive tube MPC to precisely manipulate multiple simultaneous nanowires under a coupled electric field in fluid suspension. The adaptive tube MPC estimates the unknown mobilities of the individual nanowires online, formulates dynamic tubes that update based on the online estimated mobilities and nonlinear dynamics, and addresses the coupled actuation from the global electric field with dynamic separated tubes constructed for each nanowire. The input limitation is considered during the control process, and the tube MPC formulation guarantees robust constraint satisfaction for the closed-loop system. The proposed scheme is proven to be recursive feasible and the unknown parameter set shows rapid convergence; therefore, the robustness of the system can be guaranteed. Simulation results validate the proposed algorithm that satisfies the constraints robustly and steers multiple nanowires to their targets precisely and simultaneously with accurate zeta potential estimation. We also found that the maximum disturbance that the system can reject and the manipulation time are affected by the number of the nanowires and the relative position between the nanowires; therefore, in future work, we will investigate those relations to quantify the maximum disturbance and evaluate the maximum number of nanowires that can be independently and simultaneously controlled for given disturbance bounds in experiments.

REFERENCES

Adam, G., Chowdhury, S., Guix, M., Johnson, B.V., Bi, C., and Cappelleri, D. (2019). Towards functional mobile microrobotic systems. *Robotics*, 8(3), 69.

Akin, C., Yi, J., Feldman, L.C., Durand, C., Li, A.P., Filler, M.A., and Shan, J.W. (2015). Contactless determination of electrical conductivity of one-dimensional nanomaterials by solution-based electro-orientation spectroscopy. *ACS Nano*, 9(5), 5405–5412.

Aswani, A., Gonzalez, H., Sastry, S.S., and Tomlin, C. (2013). Provably safe and robust learning-based model predictive control. *Automatica*, 49(5), 1216–1226.

Chisci, L., Garulli, A., Vicino, A., and Zappa, G. (1998). Block recursive parallelotopic bounding in set membership identification. *Automatica*, 34(1), 15–22.

Fan, D.L., Zhu, F.Q., Cammarata, R.C., and Chien, C.L. (2011). Electric tweezers. *Nano Today*, 6, 339–354.

Garcia, C.E., Prett, D.M., and Morari, M. (1989). Model predictive control: theory and practice – a survey. *Automatica*, 25(3), 335–348.

Gosse, C. and Croquette, V. (2002). Magnetic tweezers: micromanipulation and force measurement at the molecular level. *Biophys. J .*, 82(6), 3314–3329.

Grier, D.G. (2003). A revolution in optical manipulation. *Nature*, 424(6950), 810–816.

Heirung, T.A.N., Ydstie, B.E., and Foss, B. (2012). Towards dual MPC. In *Proc. IFAC Nonlinear Model Predictive Contr.*, 502–507. Noordwijkerhout, Netherlands.

Jones, T.B. (2005). *Electromechanics of Particles*. Cambridge University Press, Cambridge, UK.

Lopez, B.T., Howl, J.P., and Slotine, J.J.E. (2019). Dynamic tube MPC for nonlinear systems. In *Proc. Amer. Control Conf.*, 1655–1662. Philadelphia, PA.

Lu, X. and Cannon, M. (2019). Robust adaptive tube model predictive control. In *Proc. Amer. Control Conf.*, 3695–3701. Philadelphia, PA.

Mayne, D.Q., Kerrigan, E.C., Van Wyk, E., and Falugi, P. (2011). Tube-based robust nonlinear model predictive control. *Int. J. Robust Nonlin.*, 21(11), 1341–1353.

Mayne, D.Q., Raković, S., Findeisen, R., and Allgöwer, F. (2006). Robust output feedback model predictive control of constrained linear systems. *Automatica*, 42(7), 1217–1222.

Probst, R., Cummins, Z., Ropp, C., Eaks, E., and Shapiro, B. (2012). Flow control of small objects on chip: Manipulating live cells, quantum dots, and nanowires . *IEEE Control Syst. Mag.*, 32(2), 26–53.

Raković, S.V. and Villanueva, M.E. (2017). The maximal positively invariant set: Polynomial setting. ArXiv:1712.01150, www.arxiv.org.

Van den Heuvel, M., De Graaff, M., Lemay, S., and Dekker, C. (2007). Electrophoresis of individual microtubules in microchannels. *Proc. Natl. Acad. Sci. U.S.A.*, 104(19), 7770–7775.

Wu, J., Li, X., and Yu, K. (2020). Electrophoresis-Based Adaptive Manipulation of Nanowires in Fluid Suspension. *IEEE/ASME Trans. Mechatronics*, 25(2), 638–649.

Wu, J. and Yu, K. (2019). Adaptive Control of Nanowires Motion using Electric Fields in Fluid Suspension. In *Proc. ASME Dyn. Syst. Control Conf.* Park City, UT. Paper # DSCC2019-9051.

Yu, K., Yi, J., and Shan, J. (2015). Motion control, planning and manipulation of nanowires under electric-fields in fluid suspension. *IEEE Trans. Automat. Sci. Eng.*, 12(1), 37–49.

Yu, K., Yi, J., and Shan, J. (2018a). Automated electric-field-based nanowire characterization, manipulation, and assembly. In *Proc. IEEE Conf. Automat. Sci. Eng.*, 1612–1617. Munich, Germany.

Yu, K., Yi, J., and Shan, J. (2018b). Simultaneous multiple-nanowire motion control, planning, and manipulation under electric fields in fluid suspension. *IEEE Trans. Automat. Sci. Eng.*, 15(1), 80–91.

Yu, K., Yi, J., and Shan, J.W. (2018c). Automated characterization and assembly of individual nanowires for device fabrication. *Lab Chip*, 18(10), 1494–1503.

Yu, K., Yi, J., and Shan, J.W. (2018d). Real-time motion planning of multiple nanowires in fluid suspension under electric-field actuation. *Int. J. Intell. Robot. Appl.*, 2(4), 383–399.

Appendix A. SKETCH PROOF OF LEMMA 1

Choose $k \geq 2$, and let $\boldsymbol{M}_k^i \in \mathbb{M}_k$. For ith nanowire, let $\boldsymbol{q}_t^i$ be an arbitrary element of $\boldsymbol{R}_k^i(\boldsymbol{M}_k^i)$. Because $\boldsymbol{q}_t^i \in \boldsymbol{R}_k^i(\boldsymbol{M}_k^i)$, by the definition of $\boldsymbol{R}_k^i(\boldsymbol{M}_k^i)$ and the definition of $\boldsymbol{w}^{i^*} = [\boldsymbol{w}_0^{i^*}, \boldsymbol{w}_1^{i^*}, \cdots, \boldsymbol{w}_{k-1}^{i^*}]^{\mathrm{T}}$, we obtain

$$
\begin{aligned}
\boldsymbol{q}_t^i &= \boldsymbol{D}_{k-1}^i(\boldsymbol{M}_k^i)\boldsymbol{w}_0^{i^*} + \boldsymbol{D}_{k-2}^i(\boldsymbol{M}_k^i)\boldsymbol{w}_1^{i^*} + \cdots \\
&\quad + \boldsymbol{D}_1^i(\boldsymbol{M}_k^i)\boldsymbol{w}_{k-2}^{i^*} + \boldsymbol{D}_0^i(\boldsymbol{M}_k^i)\boldsymbol{w}_{k-1}^{i^*} \\
&= ((\boldsymbol{A}^i)^{k-1} + (\boldsymbol{A}^i)^{k-2}\boldsymbol{\theta}_{\mathrm{est}}^i\boldsymbol{B}^i M_0^i + \cdots \\
&\quad + \boldsymbol{\theta}_{\mathrm{est}}^i\boldsymbol{B}^i M_{k-2}^i)\boldsymbol{w}_0^{i^*} + ((\boldsymbol{A}^i)^{k-2} + (\boldsymbol{A}^i)^{k-3}\boldsymbol{\theta}_{\mathrm{est}}^i\boldsymbol{B}^i M_0^i \\
&\quad + \cdots + \boldsymbol{\theta}_{\mathrm{est}}^i\boldsymbol{B}^i M_{k-3}^i)\boldsymbol{w}_1^{i^*} + \cdots \\
&\quad + (\boldsymbol{A}^i + \boldsymbol{\theta}_{\mathrm{est}}^i\boldsymbol{B}^i M_0^i)\boldsymbol{w}_{k-2}^{i^*} + \boldsymbol{w}_{k-1}^{i^*}.
\end{aligned}
$$

Substitute the feedback control law $\boldsymbol{\nu}^*$ defined in Eq. (10), hence for all $\boldsymbol{q}_t^i \in \boldsymbol{R}_k^i(\boldsymbol{M}_k^i)$ and any disturbance $\boldsymbol{w} \in \mathbb{W}$,

$$
\begin{aligned}
\boldsymbol{q}_{t+1}^i &= \boldsymbol{A}^i\boldsymbol{q}_t^i + \boldsymbol{\theta}_{\mathrm{est}}^i\boldsymbol{B}^i\boldsymbol{\nu}^* + \boldsymbol{w} \\
&= ((\boldsymbol{A}^i)^k + (\boldsymbol{A}^i)^{k-1}\boldsymbol{\theta}_{\mathrm{est}}^i\boldsymbol{B}^i M_0^i + \cdots \\
&\quad + \boldsymbol{A}^i\boldsymbol{\theta}_{\mathrm{est}}^i\boldsymbol{B}^i M_{k-2}^i)\boldsymbol{w}_0^{i^*} \\
&\quad + ((\boldsymbol{A}^i)^{k-1} + (\boldsymbol{A}^i)^{k-2}\boldsymbol{\theta}_{\mathrm{est}}^i\boldsymbol{B}^i M_0^i + \cdots \\
&\quad + \boldsymbol{A}^i\boldsymbol{\theta}_{\mathrm{est}}^i\boldsymbol{B}^i M_{k-3}^i)\boldsymbol{w}_1^{i^*} + \cdots \\
&\quad + ((\boldsymbol{A}^i)^2 + \boldsymbol{A}^i\boldsymbol{\theta}_{\mathrm{est}}^i\boldsymbol{B}^i M_0^i)\boldsymbol{w}_{k-2}^{i^*} + \boldsymbol{A}^i\boldsymbol{w}_{k-1}^{i^*} \\
&\quad + \boldsymbol{\theta}_{\mathrm{est}}^i\boldsymbol{B}^i([M_{k-1}^1, \cdots, M_0^1]\boldsymbol{w}^{1^*} + \cdots \\
&\quad + [M_{k-1}^n, \cdots, M_0^n]\boldsymbol{w}^{n^*}) + \boldsymbol{w}.
\end{aligned}
$$

Applying the condition in Eq. (9), we have

$$
\begin{aligned}
\boldsymbol{q}_{t+1}^i &= \boldsymbol{A}^i\boldsymbol{q}_t^i + \boldsymbol{\theta}_{\mathrm{est}}^i\boldsymbol{B}^i\boldsymbol{\nu}^* + \boldsymbol{w} \\
&= ((\boldsymbol{A}^i)^k + (\boldsymbol{A}^i)^{k-1}\boldsymbol{\theta}_{\mathrm{est}}^i\boldsymbol{B}^i M_0^i + \cdots \\
&\quad + \boldsymbol{A}^i\boldsymbol{\theta}_{\mathrm{est}}^i\boldsymbol{B}^i M_{k-2}^i)\boldsymbol{w}_0^{i^*} \\
&\quad + ((\boldsymbol{A}^i)^{k-1} + (\boldsymbol{A}^i)^{k-2}\boldsymbol{\theta}_{\mathrm{est}}^i\boldsymbol{B}^i M_0^i + \cdots \\
&\quad + \boldsymbol{A}^i\boldsymbol{\theta}_{\mathrm{est}}^i\boldsymbol{B}^i M_{k-3}^i)\boldsymbol{w}_1^{i^*} + \cdots \\
&\quad + ((\boldsymbol{A}^i)^2 + \boldsymbol{A}^i\boldsymbol{\theta}_{\mathrm{est}}^i\boldsymbol{B}^i M_0^i)\boldsymbol{w}_{k-2}^{i0} + \boldsymbol{A}^i\boldsymbol{w}_{k-1}^{i^*} \\
&\quad + \boldsymbol{\theta}_{\mathrm{est}}^i\boldsymbol{B}^i([M_{k-1}^i, \cdots, M_0^i][\boldsymbol{w}_0^{i^*}, \boldsymbol{w}_1^{i^*}, \cdots, \boldsymbol{w}_{k-1}^{i^*}]^{\mathrm{T}}) \\
&\quad + \boldsymbol{w} \\
&= ((\boldsymbol{A}^i)^k + (\boldsymbol{A}^i)^{k-1}\boldsymbol{\theta}_{\mathrm{est}}^i\boldsymbol{B}^i M_0^i + \cdots \\
&\quad + \boldsymbol{\theta}_{\mathrm{est}}^i\boldsymbol{B}^i M_{k-1}^i)\boldsymbol{w}_0^{i^*} + ((\boldsymbol{A}^i)^{k-1} + \\
&\quad (\boldsymbol{A}^i)^{k-2}\boldsymbol{\theta}_{\mathrm{est}}^i\boldsymbol{B}^i M_0^i + \cdots + \boldsymbol{\theta}_{\mathrm{est}}^i\boldsymbol{B}^i M_{k-2}^i)\boldsymbol{w}_1^{i^*} + \cdots \\
&\quad + (\boldsymbol{A}^i + \boldsymbol{\theta}_{\mathrm{est}}^i\boldsymbol{B}^i M_0^i)\boldsymbol{w}_{k-1}^{i^*} + \boldsymbol{w}.
\end{aligned}
$$

As a result, combined with the condition in Eq. (8), we can write $\boldsymbol{q}_{t+1}^i$ as the following format: $\boldsymbol{q}_{t+1}^i = \boldsymbol{D}_{k-1}^i(\boldsymbol{M}_k^i)\boldsymbol{w}_1^{i^*} + \boldsymbol{D}_{k-2}^i(\boldsymbol{M}_k^i)\boldsymbol{w}_2^{i^*} + \cdots + \boldsymbol{D}_0^i(\boldsymbol{M}_k^i)\boldsymbol{w}$. From the above equation, we can conclude that $\boldsymbol{q}_{t+1}^i = \boldsymbol{A}^i\boldsymbol{q}_t^i + \boldsymbol{\theta}_{\mathrm{est}}^i\boldsymbol{B}^i\boldsymbol{\nu}^* + \boldsymbol{w}$ for all $\boldsymbol{w} \in \mathbb{W}$. It follows that $\boldsymbol{A}^i\boldsymbol{q}_t^i + \boldsymbol{\theta}_{\mathrm{est}}^i\boldsymbol{B}^i\boldsymbol{\nu}^* \bigoplus \mathbb{W} \subseteq \boldsymbol{R}_k^i(\boldsymbol{M}_k^i)$ with the controller $\boldsymbol{\nu}^*$ defined by Eq. (10). This completes the proof.